J. Fluid Mech. (1994), *vol.* 268, *pp.* 103–131

Dynamical properties of vortical structures on the beta-plane

By G. G. SUTYRIN†, J. S. HESTHAVEN, J. P. LYNOV AND J. JUUL RASMUSSEN

Risø National Laboratory, Optics and Fluid Dynamics Department, PO Box 49, DK-4000 Roskilde, Denmark

(Received 6 January 1993 and in revised form 24 November 1993)

The long-time evolution of monopolar and dipolar vortices influenced by the large-scale gradient of the ambient potential vorticity (the β-effect) is studied by direct numerical solutions of the equivalent barotropic quasi-geostrophic equation. Translation and reorganization of vortical structures are shown to depend strongly on their intensity. Transport of trapped fluid by vortical structures is illustrated by calculating particle trajectories and by considering closed isolines of potential vorticity and the streamfunction in a co-moving reference frame.

The initial behaviour of strong monopoles is found to be well described by a recent approximate theory for the evolution of azimuthal mode one, even for times longer than the linear Rossby wave period. In the long-time limit, strong monopoles transport particles mainly westward, although the meridional displacement is several times larger than the initial vortex size. The appearance of an annulus with opposite radial gradient of the potential vorticity around the vortex core is demonstrated. This annulus forms owing to the meridional vortex drift on the β-plane and results in reorganization of a strong monopolar vortex into a rotating tripole. A critical value of the vortex intensity is found, below which the tripolar structure does not appear even in the case of an initially shielded vortex. Weak monopolar vortices are able to trap particles and provide some west-meridional fluid transport, even in the case when they decay like a linear Rossby wave packet.

The evolution of initial f-plane dipoles on the β-plane is strongly dependent on the initial direction of propagation. Strong dipoles adjust to steadily propagating modon solutions either accelerating (westward case), decelerating (eastward case) or oscillating with a decaying amplitude (meridional case), thereby carrying trapped particles predominantly eastward. A steady state is not reached if the dipole intensity is below a critical value which depends on the initial direction of propagation. Weak dipoles either decay and shrink owing to Rossby wave radiation (westward case), gradually separate and split (eastward case), or disintegrate (meridional case) without long-distance fluid transport. Thus, on the β-plane monopoles provide mainly westward transport of trapped fluid, whereas dipoles provide mainly eastward transport. Only strong monopoles are found to provide significant meridional fluid transport.

1. Introduction

The emergence of large-scale vortical structures, remaining coherent during many turnaround times, has been recognized to be typical in quasi-two-dimensional flows

† Permanent address: Russian Academy of Sciences, P. P. Shirshov Institute of Oceanology, 23 Krasikova Street, Moscow 117218, Russia.

(e.g. Flierl 1987; McWilliams 1984, 1989). Such coherent vortices of various forms are often encountered in planetary atmospheres (e.g. Ingersoll 1990) and oceans (e.g. Kamenkovich, Koshlyakov & Monin 1986), in laboratory experiments with rotating fluids (e.g. Nezlin 1986; Hopfinger & van Heijst 1993) and in strongly magnetized plasmas (e.g. Huld *et al.* 1991). These structures may dominate the flow, trap particles and convect them over distances much larger than their initial scale size. Thus, they provide a transport, which in its nature is essentially different from classical diffusion-dominated transport. The understanding of their dynamics is therefore of great importance for the description of two-dimensional turbulence and the associated transport.

Geophysical flows are highly anisotropic due to the variation of the Coriolis parameter with the latitude. This introduces the so-called β-effect which allows Rossby wave propagation, and the wave interaction with the flow patterns may strongly affect the general dynamics. In a magnetized plasma the inhomogeneity of the plasma density allows the appearance of drift waves with properties similar to Rossby waves (e.g. Hasegawa & Mima 1978; Nycander 1989). Coherent vortex structures in plasmas are believed to be connected with anomalous transport across magnetic flux surfaces (Huld *et al.* 1991).

Two well-known types of two-dimensional coherent vortical structures are (i) the monopole with swirling velocity of the same sign everywhere and (ii) the dipole, consisting of two closely packed counter-rotating vortices. Any circular symmetric monopolar vortex is stationary in the absence of the β-effect, background flow, forcing and dissipation, implying that the monopole cannot transport fluid by itself. On the other hand, coupling of dipolar partners provides non-zero net linear momentum, causing the dipole to propagate in a direction which depends on the relative location and intensity of the two partners. Thus, without the β-effect only dipoles are able to transport particles, trapped in the central parts of the two vortices, over distances significantly larger than the size of the structure.

The dynamics of coherent vortices have been intensively studied during the last few decades, analytically, numerically and in laboratory experiments. On the β-plane the permanent-form solutions were proved to exist only with zonal direction of propagation. In the traditional quasi-geostrophic approximation such solutions with a dipolar structure having zero net angular momentum were proposed (and labelled 'modons'), first for a barotropic model by Stern (1975) and for an equivalent-barotropic model with finite radius of deformation by Larichev & Reznik (1976). General solutions, including the axisymmetric rider (Flierl *et al.* 1980), must also have a vanishing angular momentum in order to be stationary, i.e. the azimuthal velocity of the rider must change sign so that it is not a monopole. However, these solutions with riders are known to display instability (Swenson 1987). Within a more general shallow-water model, a wide class of westward-propagating anticyclonic monopoles of sizes larger than the radius of deformation is found to persist steadily (e.g. Nycander & Sutyrin 1992; Nezlin & Sutyrin 1994). Thus, steadily propagating structures on the β-plane cannot lead to any meridional transport.

Although cyclonic monopoles are not steadily propagating, neither in the quasi-geostrophic model nor in the shallow-water approximation, they may still be sufficiently long lived to be of importance for the dynamics of the flow and the associated transport (e.g. McWilliams & Flierl 1979; Sutyrin 1987). In this context, 'long lived' designates a lifetime significantly larger than the characteristic time for dispersive spreading of a linear two-dimensional Rossby wave packet of the same size. When considering the long-time evolution of a cyclonic monopole on the β-plane it is

necessary to take into account the development of the asymmetric circulation as well as the change of the symmetric vortex structure due to the meridional drift and the Rossby wave radiation.

The appearance of the azimuthal perturbation caused by the β-effect and the initial acceleration of a monopolar vortex both meridionally and westward was described by Adem (1956) using a Taylor expansion in time. For a strong monopole with separation of the timescales of the fluid rotation and the wave propagation, Sutyrin (1987) proposed an approximate theory for the evolution of the azimuthal perturbation with modenumber $l = 1$ (l is the azimuthal modenumber) during many turnaround times. It is this part of the asymmetric circulation which is responsible for the self-propelled vortex translation. This approach was successfully used by Sutyrin (1988) for describing the initial behaviour of a geostrophic point vortex and the influence of the deformation radius relative to the vortex size on the propagation of a strong Gaussian vortex on the β-plane. Detailed analysis of the translation of singular vortices on the β-plane was recently performed by Reznik (1992). For a piecewise-constant potential vorticity distribution in the vortex core, an additional vortex translation caused by distortion of the vortex shape has been described analytically by Sutyrin & Flierl (1994). However, the approximate theory for the evolution of the azimuthal mode number $l = 1$ perturbation does not allow consideration of a reorganization of the vortex structure and the long-time evolution of monopoles.

For the behaviour of strong dipoles propagating non-zonally, an approximate theory has been proposed by Nycander & Isichenko (1990). This theory is found to describe well the short-time behaviour of tilted dipoles as calculated numerically by Makino, Kamimura & Taniuti (1981) and more systematically by Hesthaven, Lynov & Nycander (1993*a*). In both studies the modon solutions, obtained by Larichev & Reznik (1976), tilted by some angle were used as the initial conditions. Note that two types of modon solutions with different structure exist: one propagating eastward with an arbitrary velocity and the other propagating westward faster than the linear Rossby waves. Investigations by Hesthaven *et al.* (1993*a*) revealed that, although different in the initial structure, both types of dipoles either end up propagating eastward with damped meridional oscillations or disintegrate, depending on their initial tilting angle and intensity. Since the dynamics of the non-stationary dipole is strongly affected by non-viscous loss of energy and enstrophy, the approximate theory fails to describe this long-time evolution.

In the present work the long-time evolution of strong and weak vortical structures on the β-plane is studied by direct numerical solutions. In §2 the basic equations are introduced and elements of the theory for propagation of strong monopolar and dipolar vortices are reviewed. In §3 we describe the numerical model and the behaviour of vortices depending on their initial structure and intensity. The development of an annulus with opposite radial gradient of the potential vorticity during the meridional displacement of the monopolar vortex and the resulting appearance of tripolar structures is emphasized. The effect of intensity and initial direction of propagation on the evolution of f-plane dipolar vortices, being steadily propagating solutions in the absence of the β-effect, is investigated. In particular, conditions for the adjustment to steadily propagating solutions are discussed. At the end of this section we discuss the transport induced by coherent structures by tracing individual massless particles and by considering closed isolines of potential vorticity and the streamfunction in a reference frame co-moving with the structure. Section 4 gives a brief summary.

2. Elements of the theory

2.1. *Model equations*

We consider the equivalent barotropic quasi-geostrophic approximation describing material conservation of the potential vorticity, q:

$$\frac{\mathrm{D}q}{\mathrm{D}t} = \frac{\partial q}{\partial t} + u\frac{\partial q}{\partial x} + v\frac{\partial q}{\partial y} = 0. \tag{1}$$

Here we adopt local Cartesian coordinates, (x, y), with positive x eastward and positive y northward. In terms of the geopotential ϕ, the geostrophic velocity (u, v) and the potential vorticity q are

$$u = -\partial\phi/\partial y, \quad v = \partial\phi/\partial x, \tag{2}$$

$$q = \nabla^2\phi - \gamma^2\phi + \beta y. \tag{3}$$

We use non-dimensional variables where the characteristic vortex size is used as the spatial scale, the parameter γ describes the ratio of the vortex size to the radius of deformation (Rossby radius) and β is proportional to the gradient of the Coriolis parameter, i.e. $\beta\gamma^{-2}$ is the non-dimensional maximum speed of the westward-propagating Rossby waves.

Equation (1) obeys the symmetry relation $\phi(x, y, t) = -\phi(x, -y, t)$. Thus, regarding monopolar vortices, we present only the evolution of cyclones, i.e. structures with positive amplitude of the potential vorticity perturbation and anticlockwise rotation.

An equation, equivalent to (1), describing the evolution of nonlinear drift waves in a strongly magnetized plasma, appears also in plasma physics. In this context the equation is known as the Hasegawa–Mima equation (Hasegawa & Mima 1978; Nycander 1989). The anisotropy is caused by a background density gradient, where ϕ designates the electrostatic potential while β is proportional to the density gradient. When analysing the propagation of vortical structures we shall use the polar coordinates (r, θ) relative to the position $(x_0(t), y_0(t))$ of the centre of the structure. In a co-moving reference frame the flow field is described by the streamfunction

$$\psi = \phi + Ur\sin(\theta - \alpha), \quad \frac{\mathrm{d}x_0}{\mathrm{d}t} = U\cos\alpha, \quad \frac{\mathrm{d}y_0}{\mathrm{d}t} = U\sin\alpha, \tag{4}$$

where $U(t)$ is the instantaneous propagation speed and $\alpha(t)$ is the angle between the direction of propagation and the eastward direction. Thus, in translating coordinates (1) becomes

$$\frac{\partial q}{\partial t} = [q, \psi], \tag{5}$$

where $[\,,\,]$ denotes the Jacobian. Note, that isolines of ψ describe the particle trajectories only in the case of a stationary flow when $q = F(\psi)$. According to (3), the fluid component of the potential vorticity is defined as

$$\xi = \nabla^2\phi - \gamma^2\phi = q - \beta y_0 - \beta r\sin\theta. \tag{6}$$

2.2. *Propagation of the monopolar vortex*

We consider two types of monopolar vortices. The first has an initial *Gaussian geopotential*

$$\phi_{init} = -\phi_m \exp(-\tfrac{1}{2}r^2), \tag{7}$$

where ϕ_m is the vortex amplitude. A cyclone ($\phi_m > 0$) of this form provides a non-monotonic profile of fluid potential vorticity with an annulus of negative fluid potential vorticity surrounding a core of positive fluid potential vorticity;

$$\xi_{init} = \nabla^2\phi - \gamma^2\phi = (2+\gamma^2-r^2)\,\phi_m \exp(-\tfrac{1}{2}r^2). \tag{8}$$

We refer to this case as a *shielded vortex*.

On the f-plane ($\beta = 0$) such vortices are prone to an azimuthal instability with mode $l = 2$ (Gent & McWilliams 1986), due to the change of sign of the radial gradient of the potential vorticity. As this instability evolves, it deforms the core into an ellipse, causing the negative potential vorticity in the annulus to collect into two satellites, thereby forming a tripole. This vortex structure has been intensively studied both numerically and experimentally during the last few years (Legras, Santangelo & Benzi 1988; Carton, Flierl & Polvani 1989; van Heijst & Kloosterziel 1989; Polvani & Carton 1990; Kloosterziel 1990; van Heijst, Kloosterziel & Williams 1991; Kloosterziel & van Heijst 1991; Orlandi & van Heijst 1992).

The β-effect causes the monopolar vortex to propagate, thereby introducing an azimuthal perturbation with mode $l = 1$. Advection of the planetary vorticity, βy, and nonlinear self-interaction of the $l = 1$ perturbation produce an $l = 2$ disturbance. Thus, on the β-plane we may expect growth of the $l = 2$ mode and consequently the emergence of a tripolar vortex. Similar behaviour was demonstrated in laboratory and numerical experiments by Kloosterziel (1990) and Carnevale, Kloosterziel & van Heijst (1991) by employing a barotropic model with a topographic β-effect and infinite radius of deformation ($\gamma = 0$).

The second case we study has an initially monotonic *Gaussian fluid potential vorticity*:

$$\xi_{init} = \xi_m \exp(-r^2), \tag{9}$$

ensuring stability of the vortex to small perturbations in the absence of the β-effect. Here ξ_m is related to the corresponding vortex amplitude in ϕ as $\xi_m = \phi_m(2+\gamma^2)$. We refer to this case as a *non-shielded vortex*.

A perturbation on the β-plane will have closed isolines of potential vorticity if $\mathrm{d}q/\mathrm{d}y|_{x=const} < 0$ along y, where $\mathrm{d}q/\mathrm{d}x|_{y=const} = 0$. For a monopolar vortex the position of the local minimum, y_c, in q is initially defined as

$$\left.\frac{\mathrm{d}\xi_{init}}{\mathrm{d}y}\right|_{x=0} = -\beta. \tag{10}$$

The radius of the vortex core, r_c, is estimated as the distance from the centre to the separatrix along $x = 0$, i.e. from the equation

$$\xi_{init}(r_c) = \xi_{init}(y_c) + \beta y_c. \tag{11}$$

Thus, for the non-shielded vortex, the location of the separatrix, y_c, along $x = 0$ is given by

$$y_c^2 = -\ln\left(\frac{\beta}{\xi_m y_c}\right).$$

The radius of the vortex core is then obtained, using (11), as

$$r_c^2 = -\ln\left[\frac{\beta}{\xi_m}\left(y_c + \frac{1}{y_c}\right)\right]. \tag{12}$$

Because of material conservation of the potential vorticity, q, fluid is expected to be

trapped in the vortex core and transported along with the vortex centre. For a strong vortex the azimuthally averaged fluid potential vorticity, $\langle\xi\rangle$, inside the vortex core decreases with increasing meridional displacement, y_0, of the vortex centre as follows from (6):

$$\langle\xi\rangle \approx \xi_{init}(r) - \beta y_0(t). \tag{13}$$

Calculation of the azimuthally averaged enstrophy inside the core yields

$$E = 2\pi \int_0^{r_c} \langle\xi\rangle^2 r\,\mathrm{d}r = E_c - 2\beta y_0 Q_c + \beta^2 y_0^2 S_c, \tag{14}$$

where

$$E_c = 2\pi \int_0^{r_c} \xi_{init}^2 r\,\mathrm{d}r, \quad Q_c = 2\pi \int_0^{r_c} \xi_{init} r\,\mathrm{d}r, \quad S_c = \pi r_c^2. \tag{15}$$

The value of E reaches a minimum for $y_0 = y_m$, where

$$y_m = Q_c/(\beta S_c). \tag{16}$$

Thus, the value of y_m gives an estimate of the maximum meridional displacement of the vortex, under the assumption that the radius of the core does not change (Larichev 1983).

From (13) we see, that even for an initially monotonic radial distribution of the potential vorticity in the vortex core, an annulus of opposite radial gradient of $\langle\xi\rangle$ may develop around the core due to the meridional drift. Thus, for an initially non-shielded monopolar vortex also, the excitation of the $l = 2$ instability and the resulting generation of a tripolar structure on the β-plane may be expected, as has been revealed numerically by Hesthaven *et al.* (1993*b*).

During a time which is less than the characteristic Rossby wave period, $T_R = 2\pi/\beta$, the evolution of the asymmetric potential vorticity, $q_a = q - \langle q\rangle$, can be described by linearizing (5) relative to the axisymmetric vortex:

$$\frac{\partial q_a}{\partial t} + \Omega \frac{\partial q_a}{\partial \theta} = b \frac{\partial \psi_a}{\partial \theta}, \tag{17}$$

$$\Omega(r) = \frac{1}{r}\frac{\mathrm{d}\phi_{init}}{\mathrm{d}r}, \quad b(r) = \frac{1}{r}\frac{\mathrm{d}\xi_{init}}{\mathrm{d}r}. \tag{18}$$

Here Ω is the angular velocity of the vortex and b describes the radial gradient of the potential vorticity.

Initially $q_a = \beta r \sin\theta$ and, following (17), the asymmetric flow around a strong vortex is represented by the azimuthal $l = 1$ perturbation in the form

$$\psi_a = r\,\mathrm{Re}\{\phi_1(r,t)\exp(-\mathrm{i}\theta)\} + Ur\sin(\theta - \alpha), \tag{19}$$

$$q_a = r\,\mathrm{Re}\{q_1(r,t)\exp(-\mathrm{i}\theta)\}, \tag{20}$$

$$\frac{\partial q_1}{\partial t} = \mathrm{i}\Omega q_1 + b(U\exp(\mathrm{i}\alpha) - \mathrm{i}\phi_1), \tag{21}$$

where $\phi_1(r,t)$ and $q_1(r,t)$ are complex functions, describing the radial structure of the $l = 1$ perturbation of the streamfunction and the potential vorticity, respectively. From (3), we obtain the relation between ϕ_1 and q_1

$$r\phi_1 = \int_0^{\infty} G(r,\rho)[\mathrm{i}\beta - q_1(\rho,t)]\rho^2\,\mathrm{d}\rho, \tag{22}$$

where

$$G(r,\rho) = I_1(\gamma r)\,K_1(\gamma\rho), \quad r<\rho,$$
$$G(r,\rho) = K_1(\gamma r)\,I_1(\gamma\rho), \quad r>\rho.$$

Here I_1 and K_1 signify the first-order modified Bessel function of the first and second kind, respectively.

When defining the vortex centre as an extremum in the fluid potential vorticity ξ, we must, in (21), set $q_1 = \mathrm{i}\beta$ at $r = 0$. This gives an expression for the propagation velocity as follows:

$$U\exp(\mathrm{i}\alpha) = \beta\frac{\Omega(0)}{b(0)} + \mathrm{i}\phi_1(0,t) = -\frac{\gamma}{2}\int_0^\infty K_1(\gamma\rho)\left(\beta\frac{b(\rho)}{b(0)}+\beta+\mathrm{i}q_1\right)\rho^2\,\mathrm{d}\rho. \tag{23}$$

This expression shows that both speed and direction of propagation depend on time. Initially $q_1 = \mathrm{i}\beta$ and $\phi_1 = 0$, implying that the monopolar vortex starts by drifting westward ($\alpha = \pi$) with a speed $U = -\beta\Omega(0)/b(0)$ according to (23). The differential rotation of the asymmetric potential vorticity (the term $\Omega\partial q_a/\partial\theta$ in (17)) and the advection of the potential vorticity of the symmetric vortex by the asymmetric flow relative to the vortex centre (the right-hand side in (17)) produces a west-meridional acceleration of the vortex centre. After many turnaround times the propagation speed approaches the maximal Rossby wave speed, $\beta\gamma^{-2}$, while the direction of propagation gradually tends to be westward. It should be noted that the solution of (21) may be expressed as $q_1 = \mathrm{i}\beta\exp(-\mathrm{i}\Omega t) + q_1'$, where q_1' describes the distortion of the vortex shape due to the asymmetric flow relative to the vortex centre.

The trajectories of the shielded and the non-shielded vortex were calculated according to (21)–(23) by Sutyrin (1987, 1988). In §3 we shall compare then with the results of our numerical solutions.

2.3. *Propagation of the dipolar vortex*

Equation (5) is known to support steadily propagating localized structures with an arbitrary functional dependence of the potential vorticity, q, on the streamfunction, ψ, inside the area of closed isolines of ψ and q. On the β-plane the quasi-geostrophic approximation is shown (e.g. Flierl 1987) to allow for permanent form solutions which propagate only in the zonal direction, either eastward ($\alpha_0 = 0$) or westward ($\alpha_0 = \pi$), where α_0 denotes the initial angle of propagation. Outside the region of closed isolines of q and ψ the unique linear relation $q/\psi = \beta/U_0\cos\alpha_0$ is defined by the unperturbed conditions far away from a localized structure. The modon solution with a linear relation $q = -(\gamma^2+\kappa^2)\psi$ inside a circular area $r < 1$ (Larichev & Reznik 1976) obeys

$$\left.\begin{aligned} &\nabla^2\phi + \kappa^2\phi = -U_0 r(\kappa^2+\rho^2)\sin(\theta-\alpha_0), && r<1,\\ &\nabla^2\phi - \rho^2\phi = 0, && r>1, \end{aligned}\right\} \tag{24}$$

where $\rho^2 = \gamma^2 + \beta/U_0\cos\alpha_0$ and $\alpha_0 = 0$ or π. Its solution takes the well-known form of a dipole vortex

$$\phi = a(r)\,U_0 r\sin(\theta-\alpha_0), \tag{25}$$

where

$$a(r) = \frac{\rho^2}{\kappa^2}\left(\frac{J_1(\kappa r)}{rJ_1(\kappa)}-1\right)-1, \quad r<1,$$

$$a(r) = -\frac{K_1(\rho r)}{rK_1(\rho)}, \qquad r>1.$$

Here U_0 is the dipole intensity which is equal to the propagation speed, U, for the steady solution, J_1 and K_1 are the first-order Bessel function of the first kind and the first-order modified Bessel function of the second kind, respectively, and κ is found as the first solution to the equation

$$\frac{\kappa J_1(\kappa)}{J_2(\kappa)} = -\frac{\rho K_1(\rho)}{K_2(\rho)}, \tag{26}$$

ensuring continuity of $\nabla\phi$ at the separatrix $r = 1$. Note that $\rho^2 > 0$ is necessary to ensure that the solution of (24) is localized, i.e. for $\alpha_0 = 0$ the propagation speed $U_0 > 0$ is arbitrary while $U_0 > \beta\gamma^{-2}$ for $\alpha_0 = \pi$. Thus, the steadily propagating dipole and the linear waves cover complementary parts of the velocity space. For the case of a strong dipole, $U_0 \gg \beta$, Nycander & Isichenko (1990) derived an approximate equation for non-zonal propagation of a tilted dipole on the β-plane. Their expression can be reduced to a simple form in terms of the propagation angle, α,

$$\frac{\mathrm{d}\alpha}{\mathrm{d}t} = -y_0 \beta U_0 \frac{S}{P_d}, \tag{27}$$

where $S = \pi$ is the area of trapped fluid inside the separatrix, y_0 is the vertical displacement of the dipole centre from the initial latitude and P_d is the magnitude of the dipole moment

$$\boldsymbol{P}_d = \int (\gamma^2\phi - \nabla^2\phi)\, \boldsymbol{r}\, \mathrm{d}x\, \mathrm{d}y, \tag{28}$$

with $\boldsymbol{r} = 0$ in the centre of the dipole vortex. Equation (27) is obtained by noting that the radius of curvature of the trajectory is equal to the ratio between the dipole moment and the monopole moment, $Q = \int \xi\, \mathrm{d}x\, \mathrm{d}y$, of the dipolar vortex, and also that the monopole moment varies linearly with the meridional coordinate as described by (13). It was assumed that the internal structure of the dipole remains unchanged, implying that S and $\boldsymbol{P}_d$ are constant, and that the radius of curvature of the trajectory is much larger than the diameter of the dipole. Validity of the assumptions were recently justified numerically by Hesthaven *et al.* (1993*a*) by varying the initial angle, but using the structure of the stationary solution, (25), for $\alpha_0 = 0$ or π as the initial conditions.

Using $\mathrm{d}y_0/\mathrm{d}t = U_0 \sin\alpha$ together with (27), gives the well-known equation of the physical pendulum. This shows that one should expect oscillatory behaviour with only small excursions from the equilibrium latitude for the eastward-propagating case, and the trajectory instability for westward-propagating dipoles ($\alpha_0 = \pi$), which has been discussed in several studies (e.g. Makino *et al.* 1981; Hobson 1991; Nycander 1992) and also recently observed experimentally on a topographic β-plane (Kloosterziel & Carnevale 1993; Velasco Fuentes & van Heijst 1994).

For $\beta = 0$ we have $\rho = \gamma$ and (25) describes the f-plane dipole, which can propagate steadily in any direction (α_0 is arbitrary) in the absence of the β-effect. This solution is a generalization of the well-known two-dimensional dipole solution of (24) in the limit of $\rho = 0$ (Chaplygin 1902; Lamb 1932), for the case of the equivalent barotropic model with finite radius of deformation. Thus, the initial structure of the f-plane dipoles does not depend on the value of β, unlike the structure of the modon solutions used by Hesthaven *et al.* (1993*a*). We consider the influence of the β-effect on such f-plane dipoles depending on the intensity U_0 and the initial angle α_0.

The evolution of the initial f-plane dipole on the β-plane is non-stationary even for zonal direction of propagation. In order to understand this we consider the meridional position of the extrema of the fluid potential vorticity, ξ, for the initial dipole, (25), with $\rho = \gamma$. The positions, $\pm y_0$, of these extrema are given as the first solution to

$$\kappa J_1'(\kappa y_0) = J_1(\kappa). \tag{29}$$

The zonal velocity at these latitudes is exactly equal to the propagation velocity, $U_0 \cos\alpha_0$,

$$-\frac{\partial\phi}{\partial y}\bigg|_{x=0} = U_0\cos\alpha_0\left(1+\frac{\gamma^2}{k^2}-\frac{\gamma^2 J_1'(\kappa y_0)}{\kappa J_1(\kappa)}\right) = U_0\cos\alpha_0. \tag{30}$$

The β-effect initially induces the westward drift of an extrema in ξ which can be calculated using the formula (Sutyrin 1988)

$$U_\beta = \beta\frac{\phi_{xx}}{\xi_{xx}}\bigg|_{y=y_0} = -\frac{\beta}{\gamma^2+\kappa^2}. \tag{31}$$

Thus, the westward-propagating dipole starts by moving faster while the eastward-propagating dipole starts by moving slower compared with the velocity on the f-plane according to the expression

$$U = U_0 - \frac{\beta}{\cos\alpha_0(\gamma^2+\kappa^2)}; \tag{32}$$

$\kappa = 3.92$ for $\gamma = 1$. Equation (32) also gives a necessary condition for initial eastward motion of the dipole, since requiring $U > 0$ for $\alpha_0 = 0$ implies

$$U_0 > \frac{\beta}{\gamma^2+\kappa^2}. \tag{33}$$

The same result may be obtained by considering the zonal velocity at the latitude of the extrema of the potential vorticity, $q = \xi + \beta y$, being shifted relative to the extrema of ξ.

Note that with the propagation speed given by (32), the relation between q and ψ remains the same, $q/\psi = -\gamma^2-\kappa^2$, inside the dipole core ($r < 1$). Outside the core, the generation of the fluid potential vorticity perturbation ξ' according to (5) is described as

$$\frac{\partial\xi'}{\partial t} = [q,\psi] = [\beta r\sin\theta, (U_0 a + U)\cos\alpha_0 r\sin\theta] = -\beta U_0\cos\alpha_0 r\frac{\mathrm{d}a}{\mathrm{d}r}\frac{\sin 2\theta}{2}, \tag{34}$$

thus producing an azimuthal mode $l = 2$ perturbation in the exterior of the dipole core due to advection of the planetary vorticity, $\beta r\sin\theta$. Using (3) we find that the corresponding initial development of the flow perturbation inside the core, $r < 1$, is described by

$$\frac{\partial\phi'}{\partial t} = \beta U_0\cos\alpha_0 F(\gamma) I_2(\gamma r)\frac{\sin 2\theta}{2}, \tag{35}$$

where

$$F(\gamma) = \int_1^\infty K_2(\gamma r)\frac{\mathrm{d}a}{\mathrm{d}r}r^2\,\mathrm{d}r = \left(\frac{2}{\gamma}+\frac{\gamma}{2}\right)K_1(\gamma) - \frac{\gamma K_0^2(\gamma)}{2K_1(\gamma)}. \tag{36}$$

The initial meridional motion of the partner centres of the f-plane dipole induced by this perturbation can be calculated by considering the meridional acceleration for, say the northern extrema in ξ, in the form

$$\frac{\mathrm{d}^2 y_0}{\mathrm{d}t^2} = F_0\beta U_0\cos\alpha_0, \quad F_0 = F(\gamma) I_2(\gamma y_0)/y_0. \tag{37}$$

Here the coefficient $F_0 \approx 0.12$ for $\gamma = 0$ and $F_0 \approx 0.08$ for $\gamma = 1$. This expression is positive for $\alpha_0 = 0$ and negative for $\alpha_0 = \pi$, implying that initially the eastward dipole

starts to split while the westward dipole starts to compress. As a result, the zonal velocity of the eastward dipole decreases whereas it increases for the westward dipole. This process has been described qualitatively and observed experimentally for the barotropic model on the topographic β-plane by Velasco Fuentes & van Heijst (1994).

Further studies of the evolution of the zonal f-plane dipoles as well as tilted ones are described in §3. The dipoles are found to display either the meridional oscillatory behaviour of strong dipoles and adjustment to the steadily propagating state or disintegration of weak dipoles by coupling to linear Rossby waves.

3. Numerical results

3.1. *Numerical model*

In order to solve (1) numerically we have employed a spectral collocation scheme (Gottlieb & Orszag 1977; Canuto *et al.* 1987) in a double periodic domain of size $L_x \times L_y$ with a resolution given by $M \times N$. An explicit third-order Adam–Bashforth predictor–corrector method is used for time integration and zero-padding is employed to remove aliasing errors. The CFL number is kept close to 0.5. The model has been tested by varying spatial and temporal resolution to ensure independence of the results on these quantities. On the f-plane a deviation of the propagation velocity of a dipole from U_0 did not exceed 1 %. On the β-plane the evolution was calculated during the time period where effects of the periodic boundary conditions were negligible owing to finite maximum phase velocity of linear Rossby waves.

Most calculations were done with a hyperviscosity term, used as a numerical filter, proportional to $\nu\nabla^6 q$ ($\nu = 10^{-16}$) added in (1) to ensure numerical stability. Our choice of hyperviscosity is dictated by a desire to confine the effects of damping to the smallest resolved scales of the model, leaving the more energetic large-scale features nearly inviscid. Employing a small Newtonian viscosity, $\nu\nabla^2 q$, ($\nu = 10^{-6}$) does not affect the large-scale properties of the vortical structures significantly. The friction influences mainly the small scales, by allowing for reconnection of isolines of potential vorticity. We observe that the hyperviscid filtering decreases the energy by less than 0.1 % and the enstrophy by only a few percent in all cases studied. Note that in purely inviscid spectral schemes the energy and enstrophy are strictly conserved ('Rugged invariants').

Passive particles are traced according to (2) by using Fourier series as the spatial interpolation scheme and an iterative second-order semi-implicit Runge–Kutta scheme for time-integration. This is a time consuming but accurate method of particle tracing, since accurate spatial interpolation of the velocity field is known to be most important for particle tracing (Yeung & Pope 1988). It was shown by Ramsden & Holloway (1991) that using an explicit fourth-order Runge–Kutta scheme did not significantly improve the trajectory prediction.

The code has been implemented and run on an Amdahl VP1200 situated at the Danish Computing Center for Research and Education (UNI•C).

3.2. *Evolution of monopolar vortices*

We have performed studies with different values of ϕ_m for the two initial conditions, (8) and (9), while keeping $\beta = 0.1$ and $\gamma = 1$ such that the characteristic linear Rossby wave period is $T_R \approx 60$. The initial conditions for the cases considered are summarized in table 1.

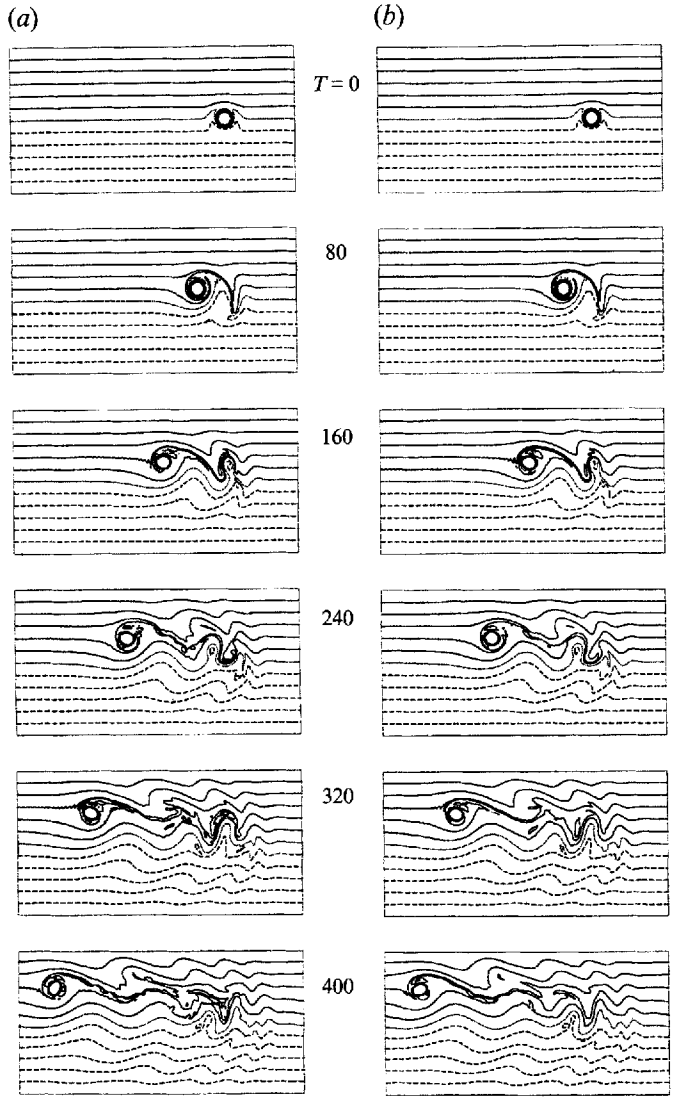

FIGURE 1. Contour plots of the temporal development of the potential vorticity q for a strong shielded vortex (Case 1 in table 1) with hyperviscosity ($\nu = 10^{-16}$) (*a*) and with Newtonian viscosity ($\nu = 10^{-6}$) (*b*).

Case	M/N	L_x/L_y	ϕ_m/β	Type	Figure
1	512/256	50/25	10.00	s	1, 4
2	512/256	50/25	10.00	n	2, 3, 4
3	512/256	50/25	2.00	s	5, 6, 16, 17
4	512/256	50/25	2.00	n	6, 7

TABLE 1. Initial parameters for the studies of monopoles. The 'Type' column indicates the shape of the initial monopole: 's' denotes a shielded vortex and 'n' a non-shielded vortex. In all cases $\beta = 0.1$ and $\gamma = 1$

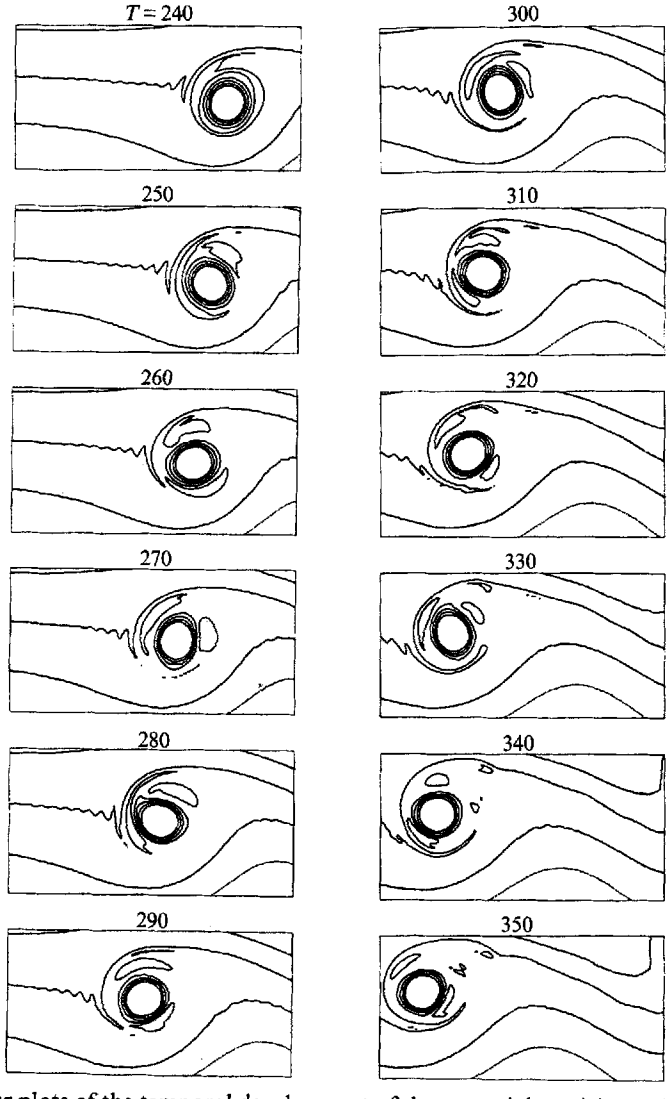

FIGURE 2. Contour plots of the temporal development of the potential vorticity, q, in the central area of the domain for a strong initially non-shielded vortex (Case 2 in table 1), showing the appearance and evolution of the non-stationary satellites.

Strong monopole

For a strong monopole ($\phi_m \gg \beta$) the development of the asymmetric circulation and translation of the vortex centre is described by (21)–(23). During the Rossby wave period, T_R, the displacement of the vortex centre is of the order of an initial vortex size and, according to (13), the change in the symmetric circulation is of the order of β (i.e a strong vortex is long-lived). In the long-time limit, $t \gg T_R$, an estimate of the meridional drift for a strong vortex according to (16) gives $y_m \sim \phi_m \beta^{-1} \gg 1$, i.e. a strong vortex may provide long-distance meridional transport.

Calculations for a shielded vortex with $\phi_m = 10\beta$ ($\xi_m = 30\beta$) show that the flow field becomes strongly asymmetric. The central part becomes elliptic at $T \approx 150$ where a tripole appears in the potential vorticity field (figure 1*a*), as expected for this initially shielded structure. However, the whole structure continues to propagate west-

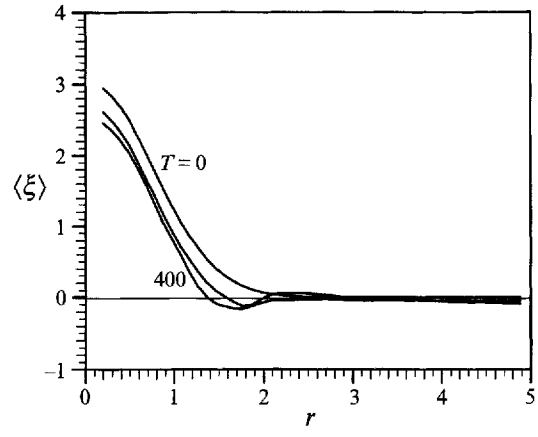

FIGURE 3. The evolution of the azimuthally averaged ξ, $\langle\xi\rangle$, for the non-shielded vortex in figure 2 (Case 2 in table 1). The profiles are given at $T = 0$, 200 and 400.

meridionally leaving a strongly nonlinear wave wake behind the vortex core. The amplitude of ϕ has decreased by about one third at $T = 400$, while ξ decreases by about 20% in agreement with (13). Thus, the decay rate of a strong vortex is significantly less than for a linear wave packet, in agreement with previous simulations by McWilliams & Flierl (1979).

Comparison with calculations using Newtonian viscosity shows that the type of viscosity only slightly affects the rotation rate of the elliptic core and behaviour of the satellites after $T = 300$ (figure 1*b*). Evidence for leaking of fluid peeled off the core into a long tendril is clear in the potential vorticity field for both calculations as it was observed for an initially shielded vortex in the laboratory and numerical simulations with a barotropic model (Carnevale *et al.* 1991). Thus, the reorganization of the initial vortex into the tripole is primarily an inviscid process, whereas the reconnection of isolines of potential vorticity clearly is a viscous effect. However, while using Newtonian viscosity the enstrophy loss is about 10% which is significantly larger than obtained with the hyperviscosity (only 3% in this case). In the remaining part of the paper, we discuss only results obtained with hyperviscous filtering.

For the initially stable non-shielded cyclone with a monotonic potential vorticity core, (9), and an amplitude of $\xi_m = 30\beta$, i.e. the amplitude of $\phi_m = 10\beta$ is the same as in the former case, the calculations show that the initially monotonic vortex core becomes elliptic and finally evolves into a tripole in the potential vorticity (figure 2), very similar to the one observed for the initially non-monotonic radial profile of potential vorticity (figure 1).

The time sequence of the potential vorticity field shown in figure 2 demonstrates that the satellites rotate in a non-stationary manner, also changing their shapes in contrast to the *f*-plane tripole (Carton *et al.* 1989), and perform a complicated motion around the elliptic vortex core, while propagating along with it. In front of the moving core the satellite is distorted and a small part of it is peeled off. Downstream of the core the satellite is restored to a nearly elliptic form before being distorted again in front of the core. The filaments appearing southward of the tripole indicate advection of ambient fluid and incorporation into the tripolar structure, thereby providing a possible mechanism for particle exchange between the vortex and the surrounding flow.

In figure 3 we have plotted the temporal evolution of the azimuthally averaged fluid potential vorticity, $\langle\xi\rangle$, of the initially non-shielded vortex. Inside the core, $r < r_c = 1.5$

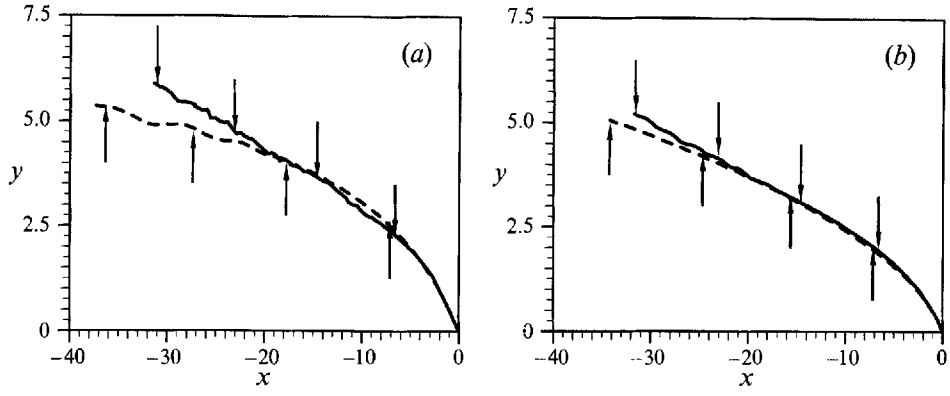

FIGURE 4. Trajectories (full lines) of a shielded vortex (*a*) and a non-shielded vortex (*b*) compared with the prediction (dashed lines) based on the azimuthal $l = 1$ perturbation theory. The initial parameters are Cases 1 and 2 in table 1. The arrows indicate the position of the vortex centre according to the numerical solution (downward pointing) and the predicted trajectory (upward pointing). The arrows are shown with a time interval of 100.

according to (12), we clearly observe that the evolution of $\langle\xi\rangle$ follows (13), i.e. the radial gradient is unaltered. Outside the core we see that the radial gradient of $\langle\xi\rangle$ changes sign and the local minimum goes below zero, similar to the initially shielded vortex. The tripole starts to emerge at $T \approx 240$, when the local minimum of $\langle\xi\rangle$ is clearly below zero, as seen in figure 3.

We suggest that the development of an annulus with opposite gradient of the potential vorticity around the vortex core is a general feature of a strong monopolar vortex on the β-plane independently of its initial structure. The resulting appearance of the observed tripole may have the same physical origin as that for f-plane tripoles, i.e. an instability of the axisymmetric vortex with non-monotonic profile of potential vorticity. However, further investigations are necessary in order to qualify this.

In figure 4 we have plotted the trajectories of the maximum ξ for the shielded as well as the non-shielded cyclones studied in figures 1 and 2 and compared the trajectories with those calculated according to (21)–(23). The position of the maximum is calculated by using a two-dimensional Taylor expansion around the position of the maximum in ξ in order to avoid problems with the discrete configuration space. It is noteworthy that, within the time of the calculations, the centres of the vortices are still quite far from reaching the expected maximum meridional displacement (for both shielded and non-shielded vortices the radius of the core $r_c \approx 1.5$ and $y_m \approx 10$). From figure 4 it is clear, however, that the vortices continue to drift meridionally, while maintaining the identity of the cores. The amplitude drop is slightly less than for the shielded vortex owing to slightly slower meridional drift. By comparing the present calculations with those for $\gamma^2 = 2$, we note that decreasing the radius of deformation (increasing γ) results in less meridional displacement (Hesthaven *et al.* 1993*b*). However, in that case the appearance of a tripolar structure from an initially non-shielded vortex was also observed.

The theory for the evolution of the $l = 1$ azimuthal mode produces trajectories which agree remarkably well for a period of time that is significantly longer than the linear Rossby wave dispersion time, $T_R \approx 60$. By comparing figure 1(*a*) to 4(*a*) and 2 to 4(*b*), respectively, it is evident that the agreement is quite good until the emergence of the tripole. In figure 4 we have also indicated the positions of the vortex at identical moments, and we observe that velocities obtained from the numerical solution and

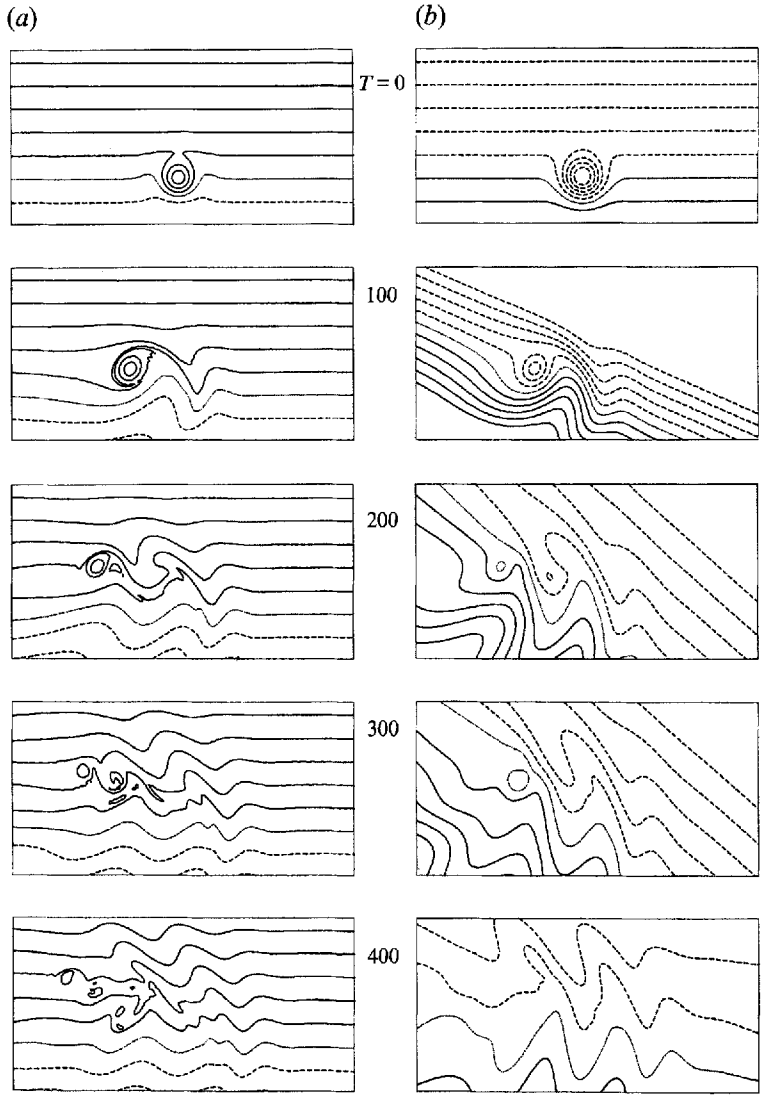

FIGURE 5. Contour plots of the temporal development of the potential vorticity, q (*a*) and the streamfunction, ψ (*b*) for a weak shielded vortex (Case 3 in table 1).

(21)–(23), respectively, are quite different for times $T > 2T_R$. This discrepancy is caused by the fact that the theory of the azimuthal $l = 1$ mode does not take into account the appearance of higher azimuthal modes and the change of the symmetric circulation. The more pronounced disagreement for the shielded vortex may be explained by observing that the appearance of the tripole occurs earlier for the shielded case than for the non-shielded case. The rotating satellites also produce some oscillations in the propagation velocity as seen in figure 4.

Evidently, the long-term evolution of a strong monopolar vortex on the β-plane does not depend on its initial structure. An annulus with opposite radial gradient of the potential vorticity appears owing to the meridional drift of the vortex centre. Splitting of the annulus into two satellites forming a tripole is, therefore, a typical features of a strong monopole.

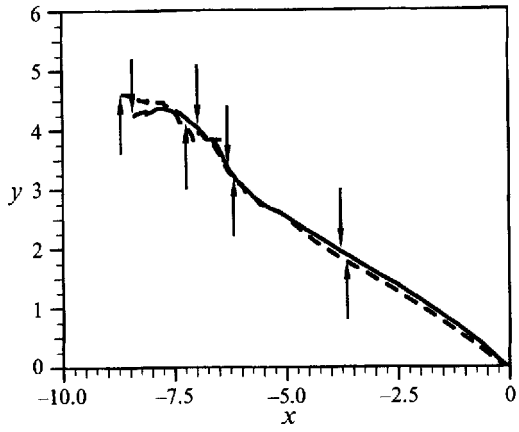

FIGURE 6. Trajectories of a weak shielded vortex (solid line) and a non-shielded vortex (dashed line) for Cases 3 and 4 in table 1. The arrows illustrates the position at different times of the non-shielded vortex (downward pointing) and the shielded vortex (upward pointing). The arrows are given with a time interval of 100.

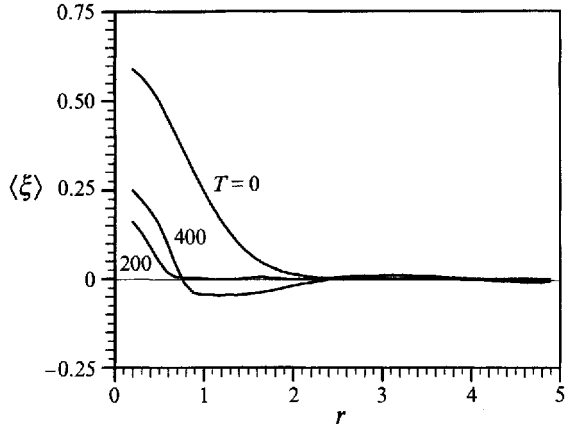

FIGURE 7. The evolution of the azimuthally averaged ξ, $\langle\xi\rangle$, for the weak non-shielded vortex (Case 4 in table 1). The profiles are given at $T = 0$, 200 and 400.

Weak monopole

By decreasing the initial vortex amplitude, the core consisting of closed isolines of q becomes smaller and the vortex decays faster owing to coupling to linear Rossby waves. Nevertheless, even for a rather weak vortex ($\phi_m = 2\beta$) which decays with a near linear rate (in ϕ, by one third at $T = T_R$), the vortex core maintains its identity for significantly longer than $T_R \approx 60$ (figure 5*a*) and even longer than the core of closed streamlines exists (figure 5*b*). Note that a tripolar structure does not appear in this case in spite of the initial presence of an annulus with negative fluid potential vorticity.

Propagation of the non-shielded vortex with the same amplitude $\xi_m = 6\beta$ ($\phi_m = 2\beta$) is very similar to that for the shielded vortex (figure 6). The numerical solution shows that an annulus of opposite radial gradient of the potential vorticity develops for this vortex as well (figure 7). However, this gradient is not steep enough for the excitation of the instability and the resulting appearance of a tripolar structure.

The initial radius of the core for both shielded and non-shielded weak vortices is $r_c \approx 1.2$ according to (10)–(12) and the maximum estimated meridional drift is $y_m \approx 3$

Case	M/N	L_x/L_y	U_0/β	α_0	Figure
1	512/256	30/15	1.00	0	8, 9
2	512/256	30/15	1.00	π	8, 9
3	256/256	15/15	1.00	$\frac{1}{2}\pi$	10
4	256/256	15/15	0.25	0	11, 12
5	512/512	15/15	0.25	π	13, 14, 16, 17
6	256/256	15/15	0.25	$\frac{1}{2}\pi$	15

TABLE 2. Initial parameters for the studies of dipoles. In all cases $\beta = 0.1$ and $\gamma = 1$

according to (16). It should be noted that y_m is derived assuming that the vortex core is unaltered. Our numerical study shows that the meridional displacement of the vortex centre becomes larger than y_m at $T \approx 3T_R$. The meridional drift continues, although slower, such that $y_0 \approx 4$ at $T \approx 5T_R$. This may be explained by observing that the shrinking of the core (figure 5) implies that the vortex propagates a longer meridional distance than estimated from (16)., The reconnection of isolines of potential vorticity is facilitated by the numerical hyperviscid filtering, which only affects the smallest scales of the potential vorticity field. Thus, even though the decay rate of the initial monopole is near linear, it still provides meridional transport of trapped particles, over a distance of the order of the initial vortex size, owing to nonlinear advection of vorticity. The transport properties of this structure will be discussed further in §3.4.

Our calculations show that the interaction between the vortex and the generated Rossby wave wake is especially important for vortices with an intermediate intensity. Their meridional displacement, being driven by a dipolar structure resulting from wave wake breaking, at the time $T = 400$ is significantly larger than in the cases of strong and weak vortices described above. Also, we found that a tripolar structure does not arise if the amplitude, ϕ_m, is less than a critical value being between 4β and 5β for both initially shielded and non-shielded monopoles. Thus, the vortex evolution depends significantly on the initial intensity rather than on the initial structure. Finally, a localized very weak perturbation ($\phi_m = 0.1\beta$) decays owing to Rossby wave radiation by one third at $T \approx 50$, in agreement with linear calculations by Flierl (1977). The flow field remains symmetric relative to the zonal direction with long waves propagating westward and short waves appearing eastward. In this low-amplitude wave case there is no core of closed isolines of potential vorticity and, consequently, there is no transport of particles.

3.3. *Evolution of dipolar vortices*

Next we consider the evolution of f-plane dipoles initially described by (25) with $\rho = \gamma$. These dipoles are known to propagate steadily in the absence of the β-effect. The reasons for using f-plane dipoles on the β-plane are, on one hand, that we wish to study the short-time modifications introduced by the β-effect and, on the other hand, to study the long-time dynamics of the most natural state of a dipolar structure as dictated by the dynamics of the system. In all calculations we again choose $\beta = 0.1$ and $\gamma = 1$. The initial conditions of the cases described are summarized in table 2.

Strong dipole

For the case of $U_0 \gg \beta$, the propagation of such a strong dipole is described by the approximate theory, (27), provided the internal structure of the dipole does not change. For considering the adjustment to the steadily propagating dipole solution we chose $U_0 = \beta$.

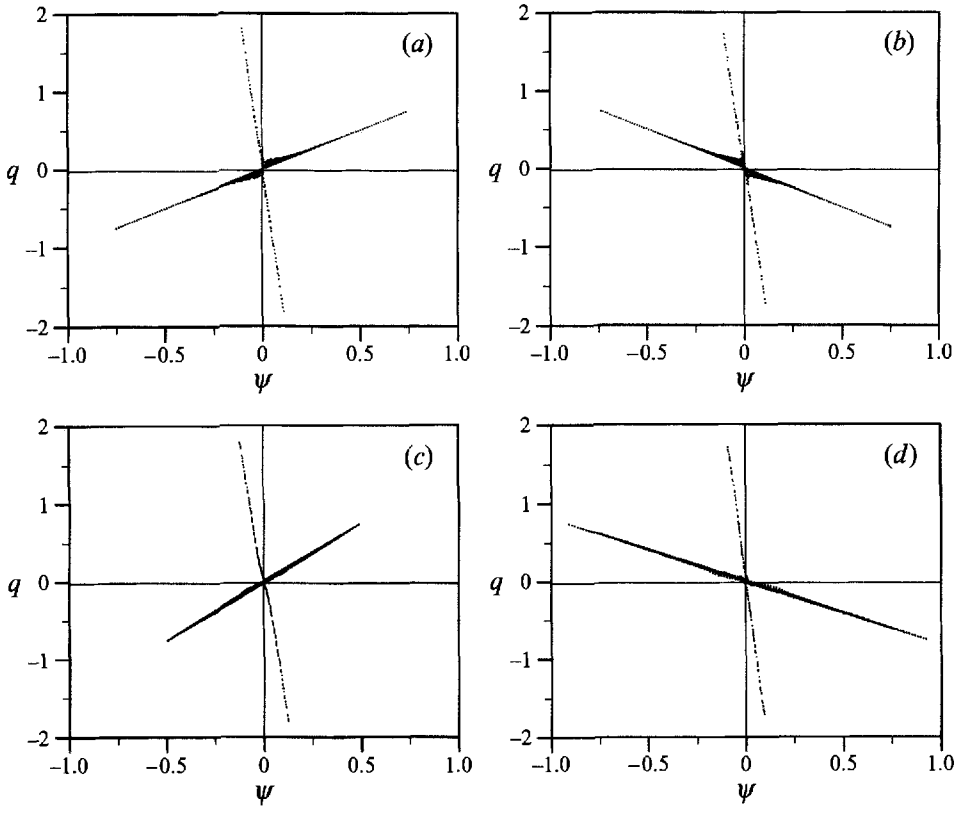

FIGURE 8. Scatter diagrams of potential vorticity, q, versus the streamfunction, ψ, for the strong eastward (a) and the strong westward (b) propagating dipoles at $T = 0$, and after adjustment to a steady state of the eastward (c) and westward (d) propagating state at $T = 200$ (Cases 1 and 2 in table 2).

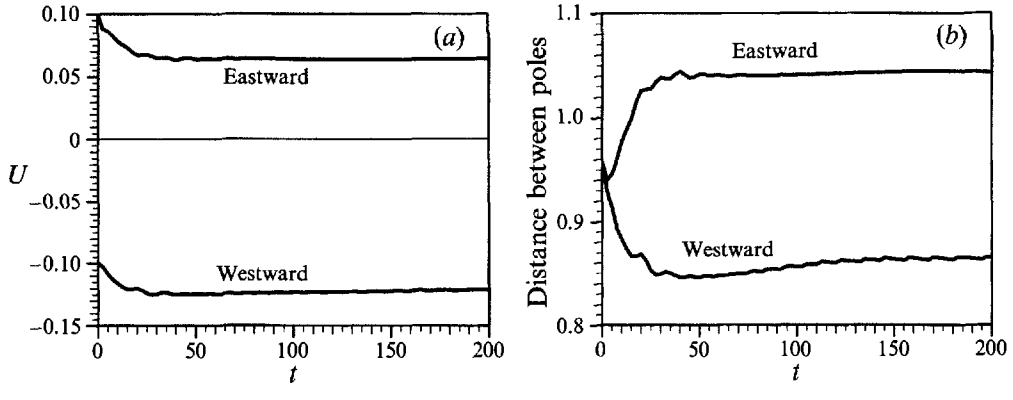

FIGURE 9. Temporal behaviour of the propagation velocity, U, (a) and the distance between the two poles (b) for the strong westward- and eastward-propagating dipoles (Cases 1 and 2 in table 2).

The initial q–ψ diagram of the zonally propagating f-plane dipoles (figure 8a, b) contains considerable scatter outside the dipole core, reflecting the non-stationarity of the structure on the β-plane. After a short time the dipoles adjust to nearly permanent-form modons, which are close to the stationary solutions given by (25). Considering the scatter diagrams of the final-state dipoles (figure 8c, d) we see in both cases that the

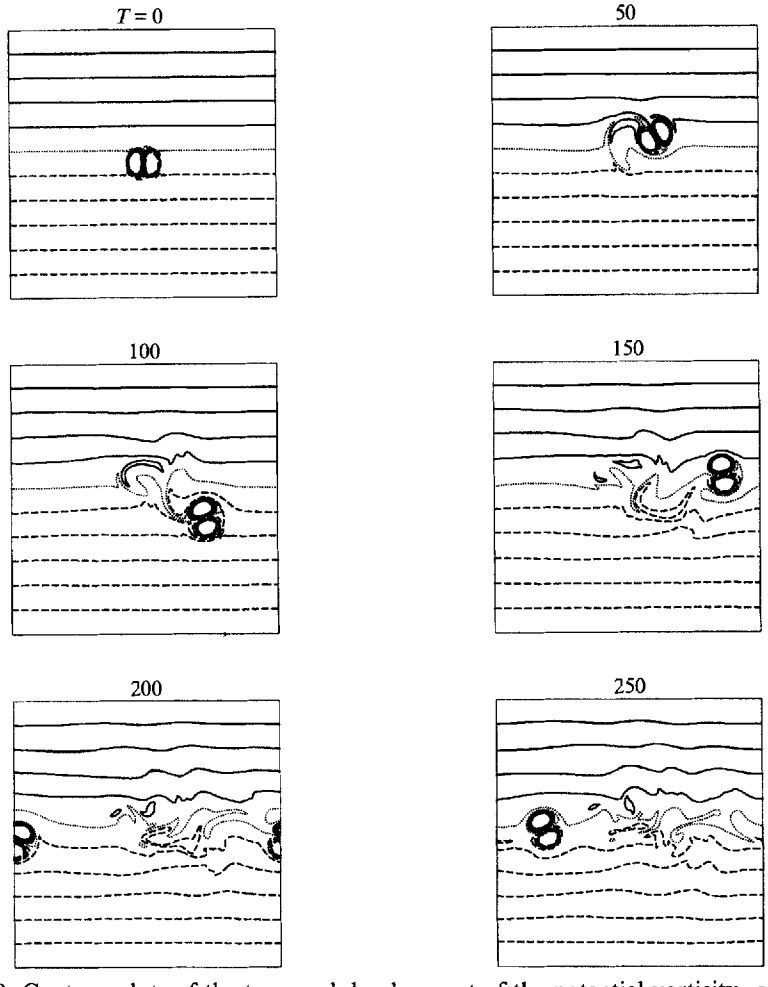

FIGURE 10. Contour plots of the temporal development of the potential vorticity, q, for a strong northward-propagating dipole (Case 3 in table 2).

sloping lines from the exterior as well as from the interior parts of the dipoles are close to being linear. The weak nonlinearity near the separatrix in the interior of eastward-propagating dipole (figure 8*c*) is related to an initial separation of the partners, thereby producing a slightly elliptical form of the separatrix in agreement with the perturbation analysis by Nycander (1988), who found a correlation between an elliptic separatrix and a cubic relation between q and ψ. For the eastward-propagating dipole we observe that the energy and the enstrophy decrease to approximately 75% of the values of the initial f-plane dipole, whereas the energy and enstrophy for the westward-propagating dipole are only a little less than the values for the initial state.

We have plotted the propagation velocity of the dipole vortex (figure 9*a*) and the distance between the centres of the vortices (figure 9*b*), illustrating the reorganization into the steadily propagating solution. For eastward direction of propagation ($\alpha_0 = 0$) the partners of the strong dipole separate slightly, in agreement with (37), resulting in an initial deceleration of the zonal motion. Correspondingly, for the westward direction of propagation ($\alpha_0 = \pi$) the partners become closer and the dipole initially accelerates. It should be noted that for the strong dipole, (33) is fulfilled even though the two dipole partners separate slightly.

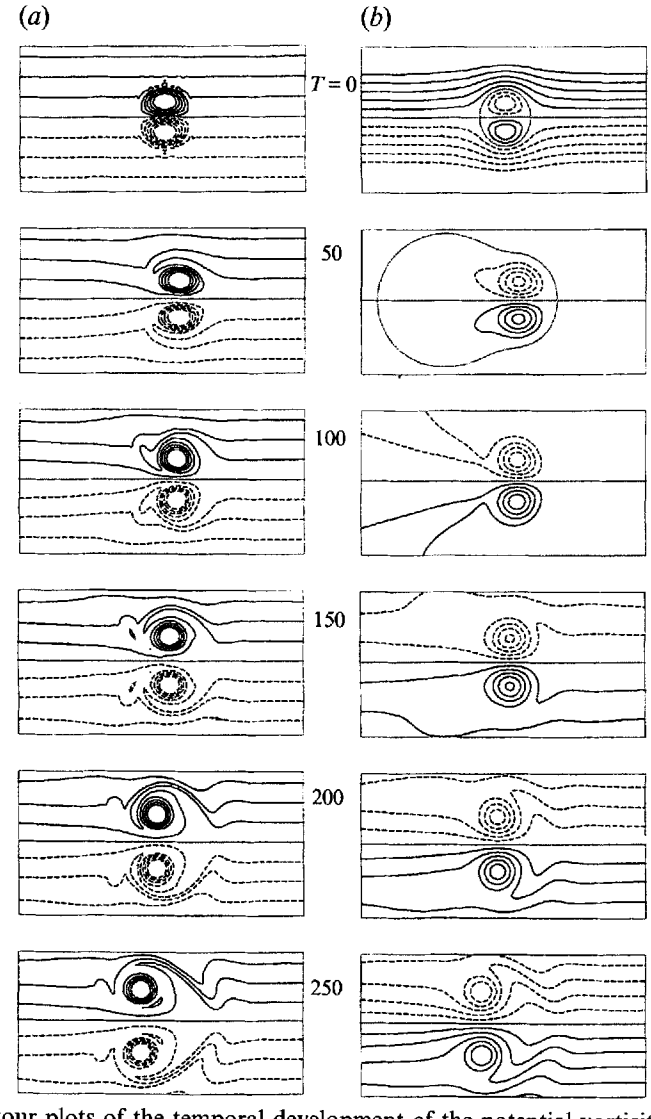

FIGURE 11. Contour plots of the temporal development of the potential vorticity, q, (*a*) and the streamfunction, ψ, (*b*) for a weak eastward-propagating dipole (Case 4 in table 2).

After the adjustment the westward dipole propagates about twice as fast as the eastward one. It does not display the trajectory instability mentioned in §2.3 since, for the exact antisymmetric flow pattern, the perturbations do not produce any of the asymmetry in the partners necessary for development of the trajectory instability. A similar adjustment to a steadily westward propagating modon without any trajectory instability was observed in numerical simulations starting from an antisymmetric pair of monopoles (McWilliams & Zabusky 1983). However, introducing a small initial deviation of the direction of propagation from westward leads to progressively increasing deviation in agreement with the stability arguments (Nycander 1992; Hesthaven *et al.* 1993*a*).

For the northward direction of propagation ($\alpha_0 = \frac{1}{2}\pi$) the strong dipole oscillates while propagating predominantly eastward (figure 10). Evidently, distortions in the surrounding field of the potential vorticity do not affect the behaviour significantly.

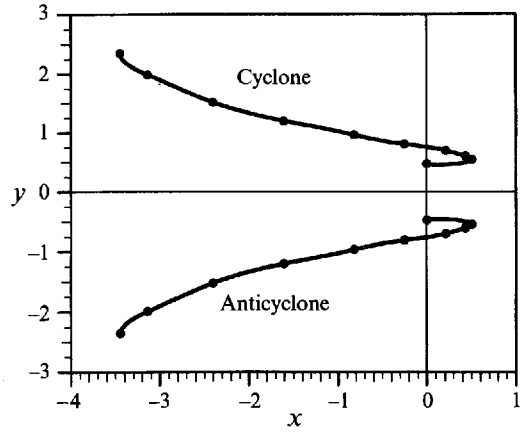

FIGURE 12. Trajectories of the two individual poles in a weak eastward-propagating dipole (Case 4 in table 2). The solid circles indicate time, with a time interval of 50.

This calculation shows that even in the case of $U_0 = \beta$ the evolution of the reorganized f-plane dipole is qualitatively explained by the theory of tilted intensive dipoles described in §2 and developed assuming $U_0 \gg \beta$ (Nycander & Isichenko 1990). This result was also obtained by Hesthaven *et al.* (1993*a*), although it was pointed out that the theory fails to describe the long-time evolution of the oscillating dipole, since the dynamics are strongly altered by the breathing of the dipole partners and non-viscous enstrophy loss.

Weak dipole

Now we consider weak dipoles with propagation speed smaller than the Rossby speed ($U_0 = 0.25\beta$).

For an eastward direction of propagation ($\alpha_0 = 0$) our calculations show (figure 11) that on the β-plane such a dipole starts by propagating eastward with the velocity $U \approx 0.2\beta$ in agreement with (32). However, shortly after the initial period we observe a slow meridional separation of the partners in the potential vorticity field (figure 11*a*) as predicted by (37). The zonal drift velocity induced in the centre of each vortex by its partner is gradually decreasing and in due course is compensated by the westward drift, typical for a monopolar vortex. Subsequently, the two vortices split apart and drift like individual monopoles, as is illustrated in figure 12, where the trajectories of the two vortices are plotted. A corresponding change in the topology of the streamfunction is seen in figure 11(*b*).

We have also indicated the temporal evolution of the dipole in figure 12. The marks clearly show that the time period of separation is relatively long. Even at $T = 200$ the amplitude of ϕ is only decreased by 3%, while the amplitude of ξ drops by 10%. Thus, such a dipolar configuration can be nearly stationary for quite a long time, displaying a particular example of a coherent structure. A similar splitting of a weak dipole was observed by McWilliams *et al.* (1981), who studied the propagation of dipoles in a random medium, as well as by Velasco Fuentes & van Heijst (1994) in their recent experimental study of dipolar vortices on a topographic β-plane with infinite radius of deformation ($\gamma = 0$). However, the dissipation in their calculations and experiments may affect the lifetime of the structure significantly.

This example illustrates that (33) is only a necessary condition for long-time

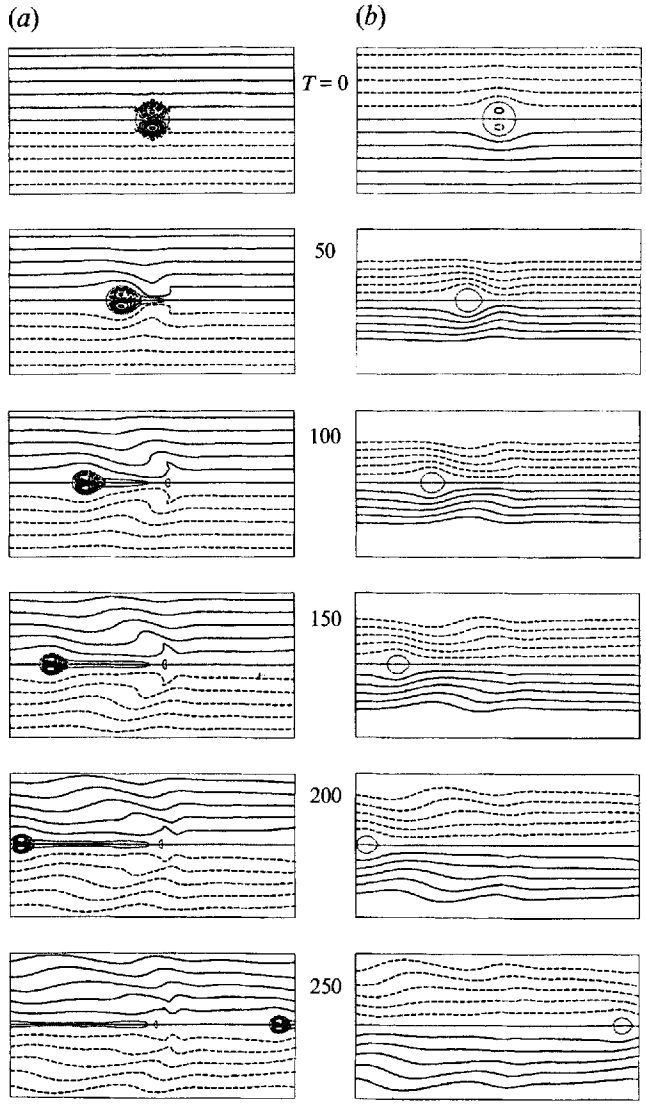

FIGURE 13. Contour plots of the temporal development of the potential vorticity, q, (*a*) and the streamfunction, ψ, (*b*) for a weak westward-propagating dipole (Case 5 in table 2).

eastward propagation, since it does not take into account the effect of the dipole separation, causing the dipole to halt and finally disintegrate into two individual monopoles which propagate while decaying like a linear Rossby wave packet of the same size. Our calculations for $\gamma = 1$ show that in order to adjust to a steadily eastward-propagating modon the initial intensity, U_0, of the f-plane dipole must exceed the critical value which is between 0.4β and 0.5β.

For the westward direction ($\alpha_0 = \pi$) the strong coupling to Rossby waves and fast decay with a nearly linear rate owing to radiation is characteristic. In the potential vorticity field we observe shrinking of the area with closed isolines (figure 13*a*) in qualitative agreement with a barotropic theory recently developed by Flierl & Haines (1993) for a strong dipole. Note that the gradient of q increases four times in the core centre due to the compressing of the partners, as is clearly seen in figure 14. The curves

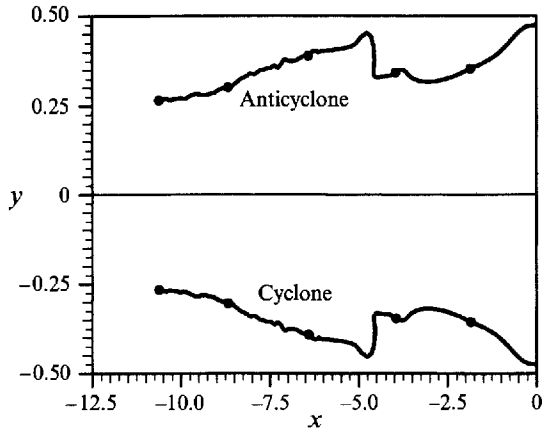

FIGURE 14. Trajectories of the two individual poles in a weak westward-propagating dipole (Case 5 in table 2). The solid circles indicate time, with a time interval of 50.

in figure 14 are trajectories of the fluid potential vorticity extrema of the two partners. The dip in both trajectories at $x \approx -5$ results from an internal shift of the location of the extrema. To resolve this behaviour, we have done the simulations with 512^2 modes and $\nu = 10^{-18}$.

Physically, shrinking of the dipole core can be explained by considering the isolines of the streamfunction, ψ, (figure 13*b*). The area of closed streamlines is slightly smaller than the core of closed isolines of the potential vorticity q owing to non-stationary compressing of the two dipole partners. As a result, the fluid near the separatrix is gradually stripped away into a fine tail behind the dipole, which leads to the observed shrinking of the dipole core. To overcome this shrinking and to adjust into a steadily westward-propagating modon requires that the intensity of the dipole exceeds a critical value which is between 0.7β and 0.8β.

For a poleward direction of propagation ($\alpha_0 = \frac{1}{2}\pi$) the calculations show a disintegration of the dipole into two structures which behave almost independently. A similar disintegration of the initial modon due to topography was observed in numerical simulations by Carnevale *et al.* (1988) with the barotropic model. It should be noted that in our case the anticyclonic partner advects some fluid southward producing a cyclonic circulation nearby (figure 15). This new dipole moves along a curved path, while the initial cyclonic partner decays as a monopole. Some meridional transport is evident from the distribution of the potential vorticity (figure 15). This configuration cannot be considered as long lived. To avoid disintegration the intensity of the northward-propagating f-plane dipole must exceed a critical value which is between 0.6β and 0.7β. This value corresponds with that found for the northward-propagating β-plane dipole with the initial structure of the eastward modon solution considered by Hesthaven *et al.* (1993*a*).

Thus, among weak dipoles which are not able to adjust to a steadily propagating state, only eastward-directed dipoles can, to some extent, be considered as long lived. Finally, a very weak dipole ($U_0 = 0.01\beta$) decays to half of its amplitude at $T \approx 200$ for an eastward as well as a westward direction of propagation. However, for the northward propagation case, the cyclonic partner decays to half of its amplitude at $T \approx T_R$, while the anticyclonic partner decays to half at $T \approx 3T_R$ owing to initial strengthing.

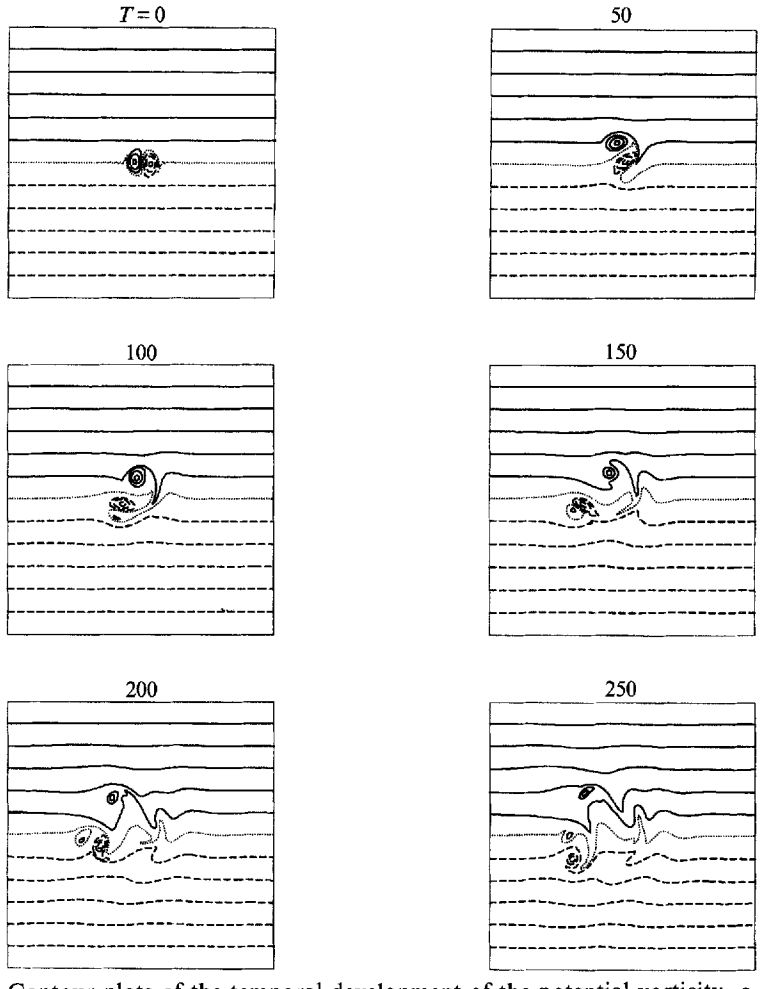

FIGURE 15. Contour plots of the temporal development of the potential vorticity, q, for a weak northward-propagating dipole (Case 6 in table 2).

3.4. *Particle dynamics and transport*

The appearance of closed isolines in the potential vorticity indicates the possibility of trapping and long-distance transport of particles. To illustrate this we have traced particles initially released near the coherent structures – inside as well as outside the core of closed isolines.

In figure 16 we have plotted trajectories in the moving reference frame of selected particles released at the meridional cross-section of a weak shielded monopole and a weak westward-propagating dipole. We observe that particles, initially released deep inside the separatrix, are effectively trapped and transported along with the structure. Particles near the separatrix leave the structure after a few rotations in the vicinity of the stagnation point of the streamfunction (see figures 5*b* and 13*b*, respectively). These results directly confirm the leaking of fluid from the core of the structure which is not so evident from the potential vorticity field. The lower part of figure 16(*b*) illustrates particle trajectories for a steadily propagating dipole on the f-plane which are close to the streamlines in this case. The slight smearing of the particle trajectories is caused by the hyperviscid filtering which implies that the steady solution becomes slightly non-stationary.

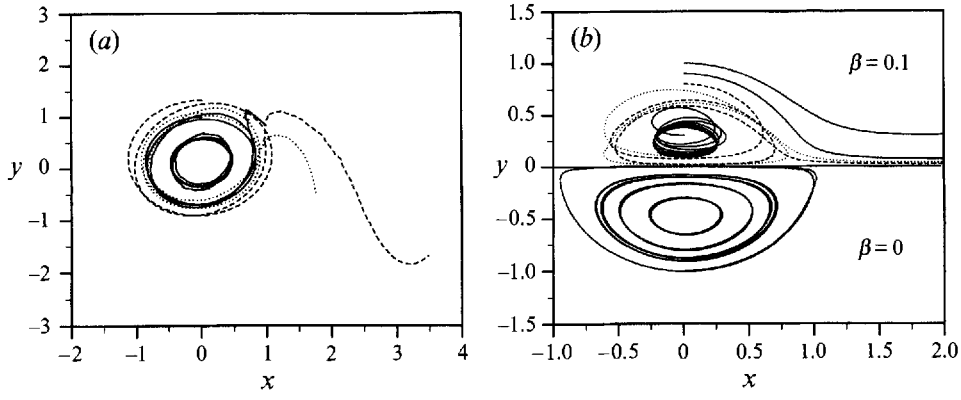

FIGURE 16. Selected particle trajectories of particles initially released around a weak monopolar vortex (*a*) (Case 3 in table 1) and a weak westward-propagating dipole (*b*) (Case 5 in table 2), lower part for a steady propagating dipole on the *f*-plane. Dotted and dashed lines illustrate particles which are lost during the propagation, whereas solid lines illustrate particles which are lost immediately or effectively trapped during the whole simulation time ($T = 250$).

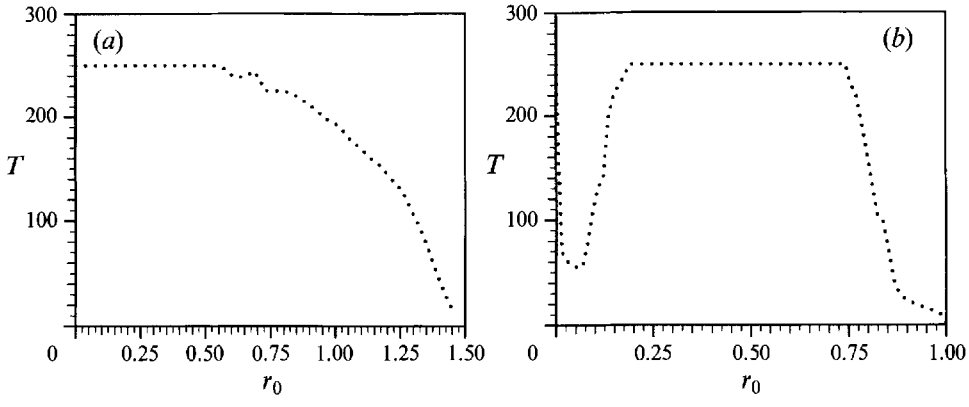

FIGURE 17. Loss rate of particles initially released at a distance r_0 from the centre of a weak monopole (*a*) (Case 3 in table 1) and a weak westward dipole (*b*) (Case 5 in table 2). T indicates the approximate time during which the particles are trapped inside the core of closed isolines of potential vorticity. The total number of particles is 150 for a monopole and 75 for the northern part of the dipole.

The relation between the size of the core of closed isolines and the ability to transport particles is illustrated by calculating the loss rate of particles released in a cross-shape around the initial monopole. The number of particles was 150. We assume the particles to be lost when the distance from the centre of the vortex is larger than $r = 1.5$.

To estimate the loss rate of particles we calculated the time during which the particles are trapped as a function of the initial distance, r_0, from the vortex centre (figure 17*a*). Here there are several interesting observations to make. Particles initially released outside the core, $r_c \approx 1.2$, are lost during $2T_R$ and are possibly never effectively trapped. Particles initially in the outer part of the core of closed isolines are lost at a nearly constant rate, whereas particles initially released in the very centre of the vortex are transported along with the vortex centre. It is noteworthy that figure 17(*a*) indicates that at $T \approx 4T_R$ approximately one-third of the particles still remained close to the position of the vortex centre. These observations clearly illustrate that the shrinking of cores of closed isolines of potential vorticity and of closed streamlines in a co-moving

reference frame allows for gradual escape of transported particles induced by the non-stationary propagation of a coherent structure. The correlation between transport and closed isolines for a non-stationary strong vortex was also discussed by Dewar & Flierl (1985) who considered passive tracer evolution.

A similar relation between cores of closed isolines in the potential vorticity and streamfunction was observed for the weak westward dipole (figure 13). In this case fluid is leaking near the rear stagnation point as indicated by calculation of the particles trajectories (figure 16*b*). The way by which fluid escapes from the non-stationary dipole as it shrinks during decay was noted also by Haines (1989) and Flierl & Haines (1993) when considering the filaments of vorticity extruding downstream from the stagnation point. The loss rate of particles calculated for this case in the same manner as for a weak monopole is shown in figure 17(*b*). It is noteworthy that particles released exactly at the inner part of the separatrix propagate to the front stagnation point and stay there. Also we observe that the fluid lost by the propagation dipole is peeled of the dipole near the separatrix and that this loss proceeds at a near constant rate.

As it has been illustrated, single conditionally released particles may provide an effective diagnostic tool to follow the dynamics of coherent structures as suggested by Pécseli & Trulsen (1989) for the investigations of coherent phase space vortices. The particle trajectories may provide information of the dynamics of the structure, its influence and amplitude (obtained from the bounce period of trapped particles).

However, no more quantitative information about the transport properties can be obtained from single-particle analysis. In order to address this question, one has to employ statistical methods on a large number of particles. When coherent structures are dominant in the flow, this becomes strongly inhomogeneous and the initial positions of the particles become crucial for the result. This implies that simple statistical methods, with for example random distribution of particles, are not sufficient, and one has to use conditional methods in order to obtain valid quantitative estimates for the transport caused by coherent structures.

4. Discussion

It has been shown that the dynamical properties of localized monopolar and dipolar vortices on the β-plane depend crucially on their intensity. The initial behaviour of strong monopoles was found to be well described, even for times longer than the linear Rossby wave period, by a recent approximate theory for the evolution of the azimuthal mode one. In the long-time limit strong monopoles transport particles mainly westward, although providing effective meridional fluid transport.

An important new feature of the evolution of a strong monopolar vortex on the β-plane is the development of an annulus with opposite radial gradient of the potential vorticity during meridional displacement of the vortex centre independently of the initial vortex structure. The resulting reorganization into a tripolar structure due to excitation of a weak instability is a general behaviour of a strong monopolar vortex if its intensity exceeds a critical value. Rotation and distortion of the tripole leads to increased mixing near the boundary of the vortex core. This mechanism will play an important role in the evolution of coherent vortices providing an exchange mechanism between the vortex core and the surrounding flow.

If the vortex intensity is below the critical level, the tripolar structure does not appear even in the case of an initially shielded vortex. The vortex core shrinks gradually during the meridional drift owing to loss of trapped fluid near the stagnation point in the streamfunction field. However, weak monopolar vortices are able to trap particles and

provide some west-meridional fluid transport, even in the case when their amplitude decays like a linear Rossby wave packet.

The influence of the β-effect on initial f-plane dipoles is strongly dependent on the initial direction of propagation. Strong dipoles adjust to steadily propagating modon solutions, either accelerating (westward case) while its partners move closer together, decelerating (eastward case) owing to slight separation of its partners, or oscillating with decaying amplitude (meridional case), thereby carrying trapped particles predominantly eastward. Weak dipoles either decay owing to Rossby wave radiation (westward case), gradually separate (eastward case), or disintegrate (meridional case) without significant long-distance fluid transport. The steadily propagating modon solutions on the β-plane are thus attractors for initial f-plane dipoles if they are strong enough.

In this study we did not change γ, the characteristic size of the structure relative to the deformation radius. Comparison of our results with calculations for smaller deformation radius (Hesthaven *et al.* 1993*b*) or infinite radius of deformation (Carnevale *et al.* 1988, 1991; Flierl & Haines 1993; Velasco Fuentes & van Heijst 1994) indicates that the main dynamical properties of the structures will not depend significantly on the deformation radius. Nevertheless, only a systematic investigation of the role of γ as compared to the results presented here would clarify effects of the deformation radius.

By tracing particles initially released inside as well as outside the core of closed isolines, we have visualized the mechanism by which fluid is lost from inside the separatrix and estimated the loss rate of trapped particles. These studies clearly illustrate that the shrinking of cores of potential vorticity and streamlines is highly correlated with the transport properties of the structure. The loss of particles has been shown to differ from the usual diffusive transport, since particles which are initially trapped deeply inside the vortex core remain trapped during the whole period of propagation.

We wish to acknowledge Lars Bækmark, Poul Michelsen and Irene Yushina for help with visualizing some of the computational data. G.G.S. gratefully appreciates the possibility of collaborating with his coauthors during his stay in the friendly and stimulating atmosphere of the Optics and Fluid Dynamics Department at Risø. J.S.H. was partly funded by UNI•C, the Danish Computing Center for Research and Education, and partly by the Danish Science Academy, which he gratefully acknowledges. This work was supported by the Danish Natural Science Research Council. We also appreciate the valuable comments by the anonymous referees which have helped us in improving the manuscript and clarifying the physical results.

REFERENCES

ADEM, J. 1956 A series solution for the barotropic vorticity equation and its application in the study of atmospheric vortices. *Tellus* **8**, 364–372.

CANUTO, C., HUSSAINI, M. Y., QUARTERONI, A. & ZANG, T. A. 1987 *Spectral Methods in Fluid Dynamics*. Springer.

CARNEVALE, G. F., KLOOSTERZIEL, R. C. & HEIJST, G. J. F. VAN 1991 Propagation of barotropic vortices over topography in a rotating tank. *J. Fluid Mech.*, **233**, 119–139.

CARNEVALE, G. F., VALLIS, G. K., PURINI, R. & BRISCOLINI, M. 1988 Propagation of barotropic modons over topography. *Geophys. Astrophys. Fluid Dyn.* **41**, 45–101.

CARTON, X. J., FLIERL, G. R. & POLVANI, L. M. 1989 The generation of tripoles from unstable axisymmetric isolated vortex structures. *Europhys. Lett.* **9**, 339–344.

CHAPLYGIN, S. A. 1902 One case of vortex motion in fluid. *Proc. Phys. Sec. Natural Phil. Soc.* **11**, 114.

DEWAR, W. K. & FLIERL, G. R. 1985 Particle trajectories and simple models of transport in coherent vortices. *Dyn. Atmos. Oceans* **9**, 215–252.

FLIERL, G. R. 1977 The application of linear quasi-geostrophic dynamics to Gulf Stream rings. *J. Phys. Oceanogr.* **7**, 365–379.

FLIERL, G. R. 1987 Isolated eddy models in geophysics. *Ann. Rev. Fluid Mech.* **19**, 493–530.

FLIERL, G. R. & HAINES, K. 1993 The decay of modons due to Rossby wave radiation. *Phys. Fluids* A (submitted).

FLIERL, G. R., LARICHEV, V. D., MCWILLIAMS, J. C. & REZNIK, G. M. 1980 The dynamics of baroclinic and barotropic solitary eddies. *Dyn. Atmos. Oceans* **5**, 1–41.

GENT, P. R. & MCWILLIAMS, J. C. 1986 The instability of barotropic circular vortices. *Geophys. Astrophys. Fluid Dyn.* **35**, 209–233.

GOTTLIEB, D. & ORSZAG, S. A. 1977 *Numerical Analysis of Spectral Methods: Theory and Applications.* SIAM.

HAINES, K. 1989 Baroclinic modons as prototypes for atmospheric blocking. *J. Atmos. Sci.* **46**, 3202–3218.

HASEGAWA, A. & MIMA, K. 1978 Pseudo-three-dimensional turbulence in magnetized nonuniform plasma. *Phys. Fluids* **21**, 87–92.

HEIJST, G. J. F. VAN & KLOOSTERZIEL, R. C. 1989 Tripolar vortices in a rotating fluid. *Nature* **338**, 569–571.

HEIJST, G. J. F. VAN, KLOOSTERZIEL, R. C. & WILLIAMS, C. W. M. 1991 Laboratory experiments on the tripolar vortex in a rotating fluid. *J. Fluid Mech.* **225**, 301–331.

HESTHAVEN, J. S., LYNOV, J. P. & NYCANDER, J. 1993*a* Dynamics of non-stationary dipole vortices. *Phys. Fluids.* A **5**, 622–629.

HESTHAVEN, J. S., LYNOV, J. P., RASMUSSEN, J. J. & SUTYRIN, G. G. 1993*b* Generation of tripolar vortical structures on the beta-plane. *Phys. Fluids* A **5**, 1674–1678.

HOBSON, D. D. 1991 A point vortex dipole model of an isolated modon. *Phys. Fluids* A **3**, 3027–3033.

HOPFINGER, E. J. & HEIJST, G. J. F. VAN 1993 Vortices in rotating fluids. *Ann. Rev. Fluid Mech.* **25**, 241–289.

HULD, T., NIELSEN, A. H., PÉCSELI, H. L. & RASMUSSEN, J. J. 1991 Coherent structures in two-dimensional plasma turbulence. *Phys. Fluids* B **3**, 1609–1625.

INGERSOLL, A. P. 1990 Atmospheric dynamics of the outer planets. *Science* **248**, 308–315.

KAMENKOVICH, V. M., KOSHLYAKOV, M. N. & MONIN, A. S. 1986 *Synoptic Eddies in the Ocean.* D. Reidel.

KLOOSTERZIEL, R. C. 1990 Barotropic vortices in a rotating fluid. PhD thesis, Utrecht University, The Netherlands.

KLOOSTERZIEL, R. C. & CARNEVALE, C. F. 1993 Propagation of barotropic dipoles over topography in a rotating tank. *Dyn. Atmos. Oceans* **19**, 65–100.

KLOOSTERZIEL, R. C. & HEIJST, G. J. F. VAN 1991 An experimental study of unstable barotropic vortices in a rotating fluid. *J. Fluid Mech.* **223**, 1–24.

LAMB, H. 1932 *Hydrodynamics*, 6th edn. Dover.

LARICHEV, V. D. 1983 General properties of nonlinear synoptic dynamics in a simple model of a barotropic ocean. *Oceanology* **23**, 410–415.

LARICHEV, V. D. & REZNIK, G. M. 1976 Two-dimensional solitary Rossby waves. *Dokl. Akad. Nauk SSSR* **231**, 1077–1079.

LEGRAS, B., SANTANGELO, P. & BENZI, R. 1988 High-resolution numerical experiments for forced two-dimensional turbulence. *Europhys. Lett.* **5**, 37–42.

MAKINO, M., KAMIMURA, T. & TANIUTI, T. 1981 Dynamics of two-dimensional solitary vortices in a low-β plasma with convective motion. *J. Phys. Soc. Japan* **50**, 980–989.

MCWILLIAMS, J. C. 1984 The emergence of isolated coherent vortices in turbulent flows. *J. Fluid Mech.* **146**, 21–42.

McWILLIAMS, J. C. 1989 Statistical properties of decaying geostrophic turbulence. *J. Fluid Mech.* **198**, 199–230.

McWILLIAMS, J. C. & FLIERL, G. R. 1979 On the evolution of isolated, nonlinear vortices. *J. Phys. Oceanogr.* **9**, 1155–1182.

McWILLIAMS, J. C., FLIERL, G. R., LARICHEV, V. D. & REZNIK, G. M. 1981 Numerical studies of barotropic modons. *Dyn. Atmos. Oceans* **5**, 219–238.

McWILLIAMS, J. C. & ZABUSKY, N. 1983 Interaction of isolated vortices. II. Modon generation by monopole collision. *Geophys. Astrophys. Fluid Dyn.* **24**, 1–22.

NEZLIN, M. V. 1986 Rossby solitons (Experimental investigations and laboratory model of natural vortices of the Jovian Great Red Spot type). *Sov. Phys. USPEKHI* **29**, 807–842.

NEZLIN, M. V. & SUTYRIN, G. G. 1994 Problems of simulations of large, long-lived vortices in the atmospheres of the giant planets (Jupiter, Saturn, Neptune). *Surveys Geophys.* **15** (in press).

NYCANDER, J. 1988 New stationary vortex solutions of the Hasegawa–Mima equation. *J. Plasma Phys.* **39**, 413–430.

NYCANDER, J. 1989 The existence of stationary vortex solutions of the equations for nonlinear driftwaves in plasmas and nonlinear Rossby waves. *Phys. Fluids* B **1**, 1788–1796.

NYCANDER, J. 1992 Refutation of stability proofs for dipole vortices. *Phys. Fluids* A **4**, 467–476.

NYCANDER, J. & ISICHENKO, M. B. 1990 Motion of dipole vortices in a weakly inhomogeneous medium and related convective transport. *Phys. Fluids* B **2**, 2042–2047.

NYCANDER, J. & SUTYRIN, G. G. 1992 Steadily translating anticyclones on the beta-plane. *Dyn. Atmos. Oceans* **16**, 473–498.

ORLANDI, P. & HEIJST, G. J. F. VAN 1992 Numerical simulation of tripolar vortices in 2D flow. *Fluid Dyn. Res.* **9**, 179–206.

PÉCSELI, H. L. & TRULSEN, J. 1989 A statistical analysis of numerically simulated plasma turbulence. *Phys. Fluids* B **1**, 1616–1636.

POLVANI, L. M. & CARTON, X. J. 1990 The tripole: a new coherent vortex structure of incompressible two-dimensional flows. *Geophys. Astrophys. Fluid Dyn.* **51**, 87–102.

RAMSDEN, D. & HOLLOWAY, G. 1991 Timestepping Lagrangian particles in two dimensional Eulerian flow fields. *J. Comput. Phys.* **95**, 101–116.

REZNIK, G. M. 1992 Dynamics of singular vortices on the beta-plane. *J. Fluid Mech.* **240**, 405–432.

STERN, M. 1975 Minimal properties of planetary eddies. *J. Mar. Res.* **33**, 1–13.

SUTYRIN, G. G. 1987 The beta-effect and the evolution of a localized vortex. *Sov. Phys. Dokl.* **32**, 791–793.

SUTYRIN, G. G. 1988 Motion of an intense vortex on a rotating globe. *Fluid Dyn.* **23**, 215–223.

SUTYRIN, G. G. & FLIERL, G. R. 1994 Intense vortex motion on the beta-plane: Development of the beta-gyres. *J. Atmos. Sci.* **51** (in press).

SWENSON, M. 1987 Instability of equivalent-barotropic riders. *J. Phys. Oceanogr.* **17**, 492–506.

VELASCO FUENTES, O. U. & HEIJST, G. J. F. VAN 1994 Experimental study of dipolar vortices on a topographic β-plane. *J. Fluid Mech.* **259**, 79–106.

YEUNG, P. K. & POPE, S. B. 1988 An algorithm for tracking fluid particles in numerical simulations of homogeneous turbulence. *J. Comput. Phys.* **79**, 373–416.